

The Influence of Field-Aligned Currents on Electron Density in the Ionosphere: Combined Observations of *SWARM* Satellites and ESR Radar

R. Yu. Lukianova*

Space Research Institute, Moscow, 105064 Russia

*e-mail: renata@aari.ru

Received February 28, 2023; revised March 22, 2023; accepted March 24, 2023

Abstract—The results are presented of combined measurements by the *SWARM* spacecraft (SC) and European incoherent scatter radar on Svalbard for two events of simultaneous observations: in the nighttime ionosphere during substorm activation on January 9, 2014, and in the daytime ionosphere under quiet conditions on February 5, 2017. Onboard magnetometers of the *SWARM* SC provide measurements of field-aligned current density over the ionosphere. The radar, which is under the flyby trajectory at this time, measures the vertical distribution of the electron density (Ne). Experiments have shown that, under disturbed nighttime conditions, at the location of the field-aligned current flowing from the ionosphere, the plasma density increases throughout the entire slab of the ionosphere and the change in Ne is in agreement with theoretical estimates. In the daytime quiet ionosphere, Ne increases only in the *F* layer, but practically does not change in the *E* layer. The differences may be due to the fact that, in the first case, the carriers of the upward directed current are represented by the entire energy spectrum of auroral electrons of 1–10 keV, and in the second case only by the low-energy part.

DOI: 10.1134/S0010952523700454

INTRODUCTION

Field-aligned electric current (FAC) that flows along geomagnetic-field lines \mathbf{B} plays a major role in the transfer of energy between the solar wind, the magnetosphere, and the ionosphere. Satellite observations have revealed the global distribution of FAC in the ionosphere and also made it possible to determine the mechanisms of FAC generation in the magnetosphere. The large-scale FAC system includes region 1 currents, which connect the outer layers of the magnetosphere with the high-latitude ionosphere, and region 2 currents located more equatorially, which connect the inner magnetosphere with the auroral ionosphere [1]. The density of large-scale FAC is typically on the order of $1 \mu\text{A}/\text{m}^2$. However, the current sheets are inhomogeneous; they contain currents of small spatial scales, but of high intensity, on the order of $10\text{--}100 \mu\text{A}/\text{m}^2$ [2, 3].

FAC carriers are electrons with low mass and high mobility along \mathbf{B} . Upwardly directed (outflowing from the ionosphere) FAC correspond to the decrease of electron heat flux, while FAC flowing into the ionosphere are accompanied by outgoing electrons. In the region of FAC, an increase in the electron density and a corresponding increase in conductivity occur. In the region of the inflowing FAC, the decreases. To close the ionospheric current connecting regions with dif-

ferent conductivities, the electric field at the downward FAC must be greater than at the upward one. This phenomenon is considered one of the common features of aurora arcs and has been observed using a combination of optical methods with radar and satellite measurements (e.g., [4, 5]). In the ionosphere, FAC are closed due to Pedersen currents, the carriers of which are mainly ions. Thus, a three-dimensional current system arises, and a local change in the plasma density should occur in the region of the downward and upward FACs in the ionosphere.

Theoretical estimates of changes in the electron density (Ne) were made on the basis of solving the equations for the motion of the ionospheric plasma and the closure of currents [6–8]. However, over the years that have passed since the appearance of these works, experimental confirmation of this effect has not appeared. This is due to the fact that, in the experiment, it is necessary to have data on simultaneous measurements of the FAC density and the Ne vertical profile. Direct measurements of the FAC over the ionosphere can only be carried out with the help of low-orbit spacecraft (SC), and the height distribution of Ne can only be obtained with the help of an incoherent scatter radar, which is at that time under the flyby trajectory. Since in fact there are only two high-latitude incoherent radars—on the Spitsbergen archipel-

ago and in Alaska—and at present only the *SWARM* SCs are in polar orbit, and these two measuring instruments do not conduct coordinated experiments, it is very difficult to provide the desired combination of observations. However, using the open database of European radar measurements ESR and *SWARM* SC, it was possible to select several representative events. The purpose of this work is to study the influence of the FAC on the electron density profile using combined observations of the spacecraft *SWARM* and EISCAT ESR radar (European Incoherent Scatter Scientific Association—EISCAT Svalbard Radar) during selected representative events.

1. *SWARM* SATELLITES AND INCOHERENT SCATTER RADAR ESR

The *SWARM* mission, consisting of three identical spacecraft, has been in low polar orbit since 2014. Two spacecraft, *SW-A* and *SW-C*, fly at an altitude of 420 km parallel to each other at a distance of 0.5° – 1.5° in longitude, with the orbital inclination being 87.4° . The orbit of the third spacecraft, *SW-B*, lies in another meridional plane (an inclination of 88°) at an altitude of 500 km. Gradually shifting for 7–10 months, satellite trajectories cover all longitudinal sectors of the globe. All three *SWARM* SC are equipped with identical hardware. The main module is a complex for magnetic measurements: highly sensitive vector and scalar magnetometers for determining the magnitude and direction of the total vector and geomagnetic-field variations with an accuracy of 0.1 nT and a frequency of 1 Hz. At high latitudes, a vertically directed current creates a magnetic field the vector of which lies in the horizontal plane. If the spacecraft trajectory crosses the FAC, the onboard magnetometer, in addition to the main field, measures magnetic variations, from which the current density is calculated. The FAC density calculated according to the standard algorithm [9] is one of the parameters included in the *SWARM* database. In addition to the magnetometric equipment, spacecraft are equipped with Langmuir probes for measuring the density and temperature of the electronic component of the ionospheric plasma. *SWARM* data, structured by daily files, are presented on the website of the European Space Agency.

Radars of the European scientific system EISCAT are designed to study the ionosphere by emitting a radio signal at 500 MHz and receiving a backscatter signal, which can be used to draw a conclusion about the physical parameters of the ionosphere, such as the characteristics of Ne, the temperature of electrons and ions, the speed of ions on the line of sight in the range from 90 to 400 km. The northernmost of the radars, ESR (European incoherent radar), is located on the Svalbard archipelago (78.2° N, 16° E). It measures the characteristics of the ionospheric plasma near the polar-cap boundary. The system consists of two antennas: one with a diameter of 42 m is fixed and

directed along the local line of the geomagnetic field (azimuth 184° , inclination angle 82.1°); the second, with a diameter of 32 m, is fully steerable. Periodically, a large antenna performs measurements according to the general CP program (ipy mode). In this mode, series of altitude profiles of ionospheric parameters are obtained when sounding along the geomagnetic field line. To estimate the density and temperature of electrons, the temperature and velocity of ions within the line of sight of the beam with a resolution of 1 min at altitudes of 100–400 km are divided into 32 ranges, the standard GUISDAP software is used [10]. The MADRIGAL online database contains observational data from ESR sessions since 1996.

2. RESULTS OF RADAR AND SATELLITE OBSERVATIONS

To search for events of combined satellite measurements of the FAC and radar measurements of the Ne vertical profile from the *SWARM* database of flyby trajectories were selected passing over the ESR location at a distance of no more than 2° in latitude (~ 60 km). The ESR database was then checked for these events to see if there were 42-m antenna sessions at that time. In this section, we consider two representative events of combined measurements, one of which (February 5, 2017) occurred in a magnetically quiet period, and the second (January 9, 2014) during substorm activation. Figure 1 shows the values for these 2 days of the local auroral electrojet index (EI), which is calculated from the data of the Scandinavian meridional chain of IMAGE magnetometers.

2.1. Event of February 5, 2017

On this day, the trajectory of the flight of the tandem spacecraft *SW-A* and *SW-C* passed near the ESR location at 1520–1530 UT. *SW-C* was 4 s ahead of *SW-A* and was approximately 1° of longitude closer to the radar beam. Figure 2 shows a part of the spacecraft tandem flight trajectory in a rectangle bounded by geographic coordinates 65° – 85° N and 5° – 27° E latitude (Fig. 2a), as well as the polar projection of the trajectory in geomagnetic coordinates (Fig. 2b). The polar projection is superimposed on the pattern of large-scale FACs obtained from the data of *Ampere* (Active Magnetosphere and Planetary Electrodynamics Response Experiment). Within the framework of the *Ampere* project, maps of the FAC density distribution in the high-latitude region with a 10-min resolution are available through the web portal. The maps are based on measurements of magnetic-field variations by engineering magnetometers of the satellite constellation *Iridium Communications*, which consists of more than 70 spacecraft in a circumpolar orbit [11]. It can be seen from Fig. 2b that a large-scale upward FAC with a density of up to $0.6 \mu\text{A}/\text{m}^2$ is located south of Svalbard. The *SW-A* and *SW-C* SC fly near the

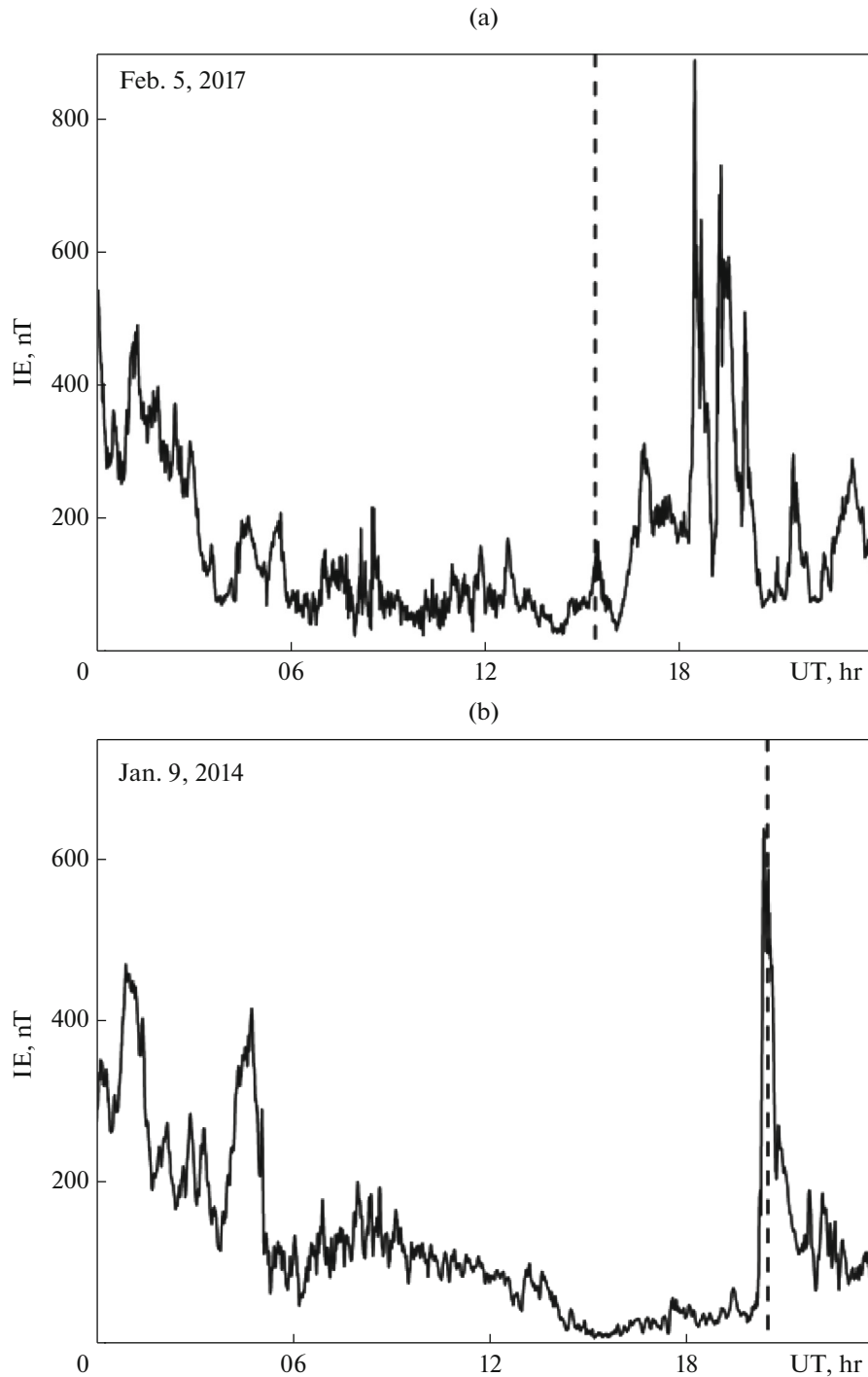


Fig. 1. EI for February 5, 2017, and January 9, 2014. Vertical dotted lines show the moments of the location of the *SWARM* SC above the ESR radar.

ESR beam approximately at the middle of the minute 15:23 UT, and the zone of the downward FAC enters at the end of this minute.

Parameters of the longitudinal electric current calculated from the measurements of the onboard magnetometers of the *SW-A* and *SW-C* SC are pre-

sented in Fig. 3. To reveal large-scale structures, the initial 1-Hz values were averaged over 31 points. Observations of both satellites indicate that a large-scale downward (considered positive) FAC with a density of up to $0.8 \mu\text{A}/\text{m}^2$ is located approximately between 66° and 70° latitude, with the upward (considered negative) of slightly less density being between

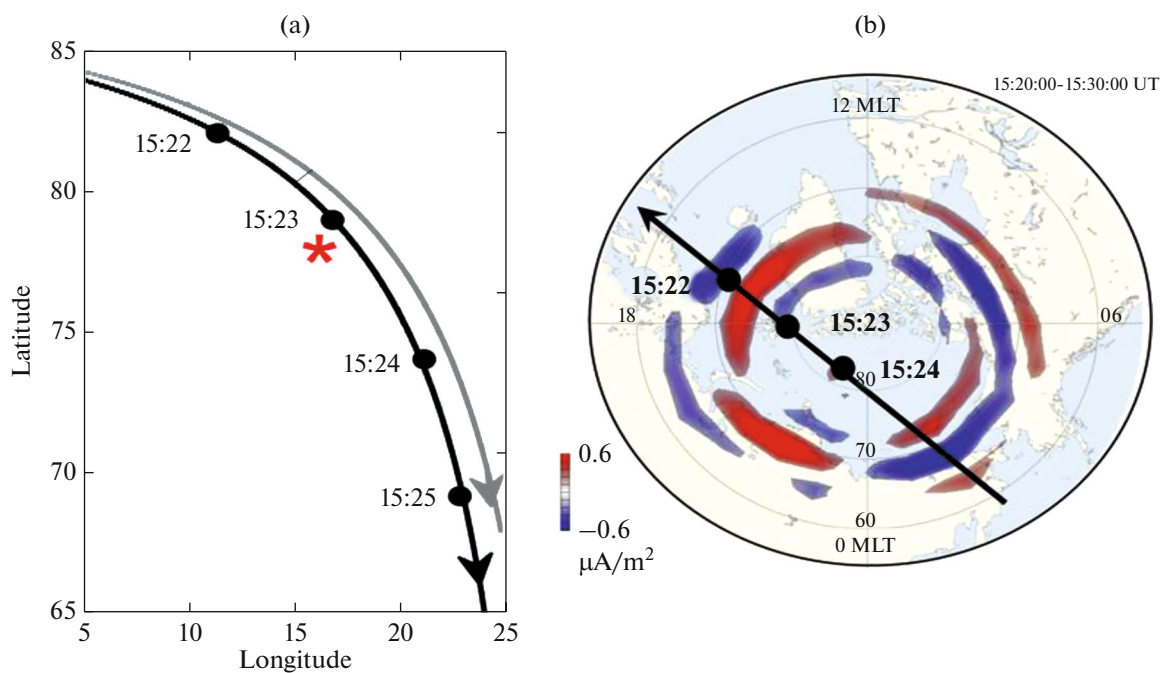


Fig. 2. (a) Spacecraft flyby trajectories of *SW-A* (gray line) and *SW-C* (black line) at 15:22–15:25 UT on February 5, 2017; geographical coordinates; the asterisk indicates the location of the ESR radar. (b) FAC ionospheric projection according to *Ampere* data (red color is the current flowing out of the ionosphere, blue color is the current flowing into the ionosphere), averaged over the interval 15:20–15:30 UT, and the SC flyby trajectory (black line and minute reference points); local geomagnetic time (MLT)–geomagnetic longitude coordinates.

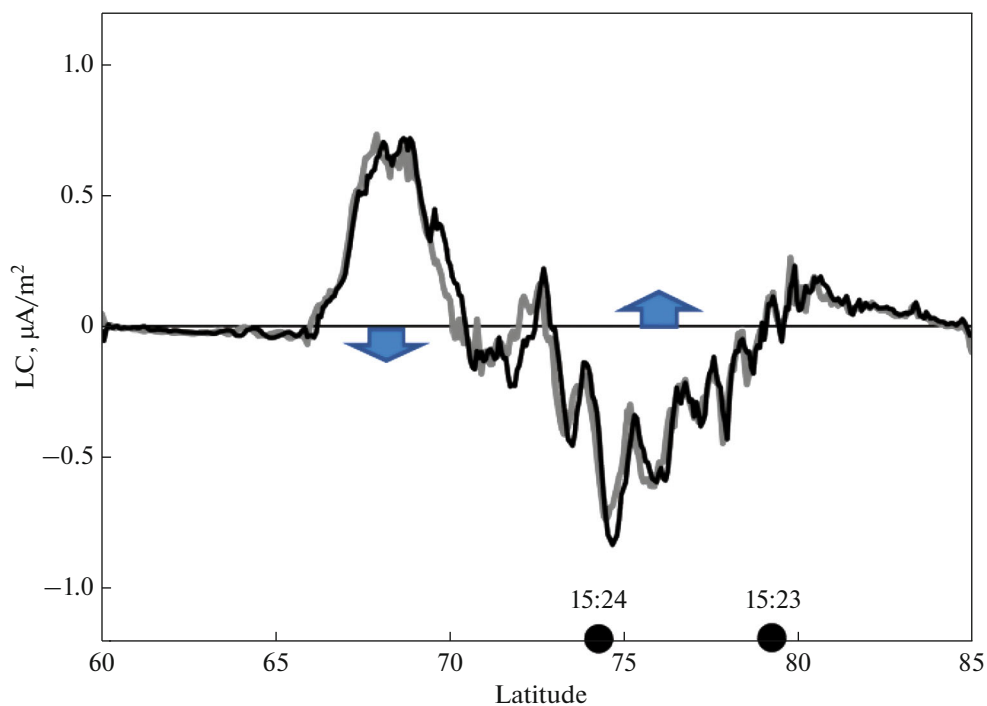


Fig. 3. FAC density according to measurements of *SW-A* (gray line) and *SW-C* (black line) SC for February 5, 2017. An arrow pointing down (up) denotes the FAC inflowing into the ionosphere (outflowing from the ionosphere). Dots on the *X*-axis indicate minutes when the *SW-C* SC was close to the ESR.

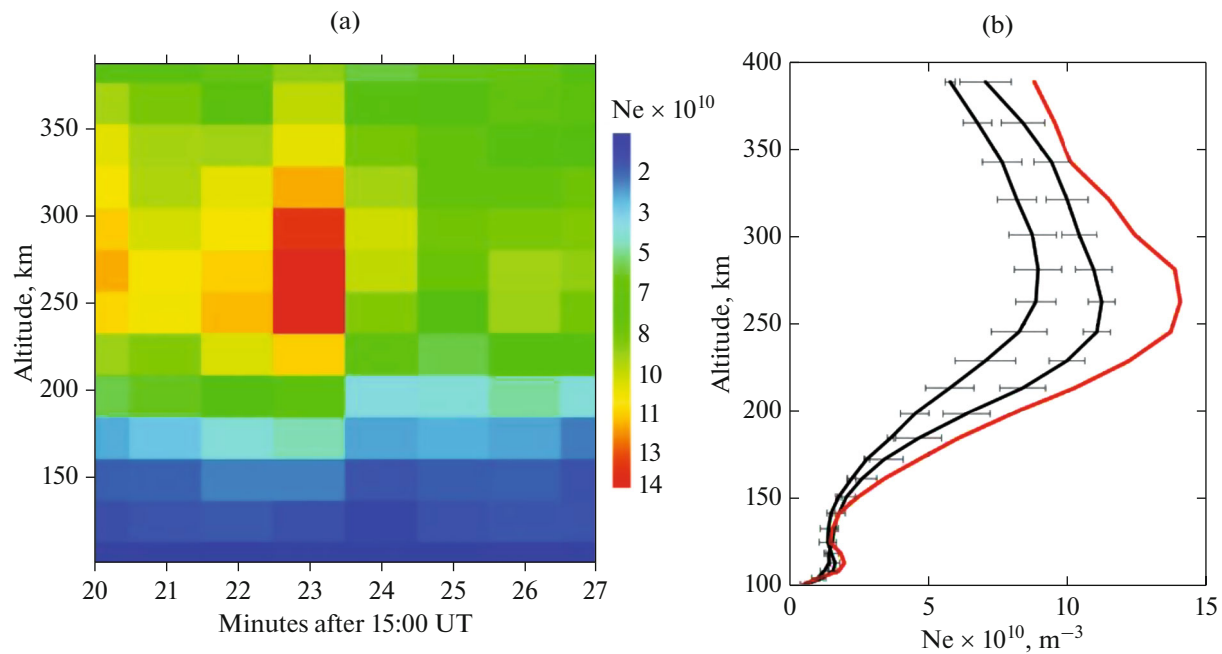


Fig. 4. (a) Altitude distribution of Ne at 15:20–15:27 UT on February 5, 2017; (b) Ne vertical profile at 15:23 UT (red line) and profiles averaged over the three previous and three subsequent minutes (lines with standard deviation).

73° and 79°. Instantaneous (1 s) FAC values reached $4 \mu\text{A}/\text{m}^2$. The segment of the spacecraft trajectory closest to the radar is in the zone of the current flowing from the ionosphere.

On this day, radar observations were carried out according to the SR program in the ipy mode from 13:00 to 18:00 UT. Figure 4a shows 1-min Ne vertical profiles measured from 15:21 to 15:28 UT. It can be seen that, at 15:23, at heights of the *F* layer of 250–300 km, there is a sharp increase in Ne to $1.4 \times 10^{11} \text{ m}^{-3}$. A slight increase in density is noticeable even lower, in the range of 170–220 km. The moment of time corresponds exactly to the crossing by the satellites of the zone of the FAC, which flows out of the ionosphere. To quantify the change in Ne, three profiles are distinguished in Fig. 4b: a central one at 15:23 UT and ones averaged over the three previous and three subsequent minutes. The difference between the central and neighboring, previous and subsequent, profiles in the Ne maximum at an altitude of 260 km is, respectively, 2.5×10^{10} and $7 \times 10^{10} \text{ m}^{-3}$. Differences are noticeable both at high and low altitudes. In the *E* layer, they are equal to several tenths of a unit.

It should be noted that the averaging of radar and satellite data introduces some uncertainty into the result of their comparison. On the high *F* layer, the diameter of the volume observed by the radar is about 2 km and the tilt of the beam shifts the area of illumination by about 50 km to the south of the antenna location. In the zonal direction, the radar rotates along with the Earth at a speed of about 15 km/min and the beam can gradually leave the area occupied by the

FAC. The integration time of the radar data required to obtain an acceptable signal-to-noise ratio is 1 min. The length of the projection of a 1-min segment of the trajectory of a satellite flying along the meridian is about 200 km. It is obvious that the spatially and temporally averaged radar measurements do not necessarily correspond to any of the small-scale forms of FAC observed from the satellite. However, if the FAC maintains its main direction (inflowing or outflowing current) during the minute over which Ne is averaged, the comparison can be considered quite correct.

2.2. Event of January 9, 2014

On this day, the passage of satellites over the radar operating in the SR mode coincided with the peak of substorm activation, and the trajectory passed through the premidnight sector of local time. At 20:29 UT, under disturbed conditions, the FAC structure, especially the small-scale one, is unstable and can change rapidly. Figure 5 shows a part of the flight trajectory of the *SWARM* SC near the ESR beam (Fig. 5a) and the polar projection of large-scale FAC along *Ampere* (Fig. 5b). At the beginning of the *SWARM* mission, before the start of the orbit separation procedure at the end of winter 2014, all three spacecraft flew close to each other. Therefore, graphically, the trajectories *SW-A* and *SW-C* combined in one line. The *SW-B* trajectory passes slightly to the east, and this spacecraft is ahead of the tandem by a few seconds. The averaged pattern of FAC in Figs. 5b shows that, at the trajectory point at 20:29 UT, the ESR is in the region of a stratified large-scale upward FAC. At 20:30 UT,

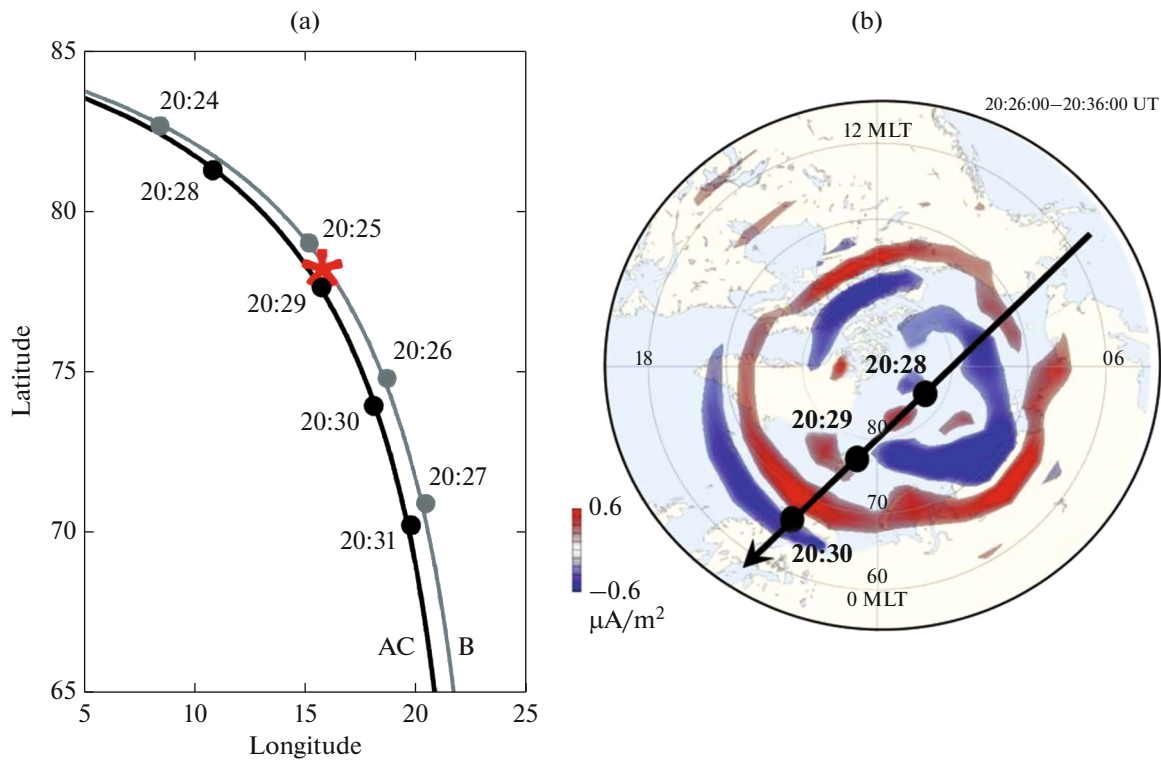


Fig. 5. (a) Flyby trajectories and minute reference points for *SW-A* and *SW-C* (common black line) and *SW-B* (gray line) January 9, 2014, in geographic coordinates; the asterisk indicates the location of the ESR radar; (b) the ionospheric projection of the FAC over *Ampere* (red color is the FAC flowing out of the ionosphere, blue color is the FAC flowing into the ionosphere), averaging over 20:26–20:36 UT and the SC flyby trajectory (black line); MLT—geomagnetic longitude coordinates.

the spacecraft cross the outflowing current zone. As the Earth rotates and a substorm develops, the position of the radar can move back and forth between regions 1 and 2 with FAC in the opposite direction. Flying through the nighttime part of the auroral zone, satellites observe many small-scale structures embedded in large-scale FACs.

Figure 6 shows the current densities averaged over 31 points according to the *SW-C* and *SW-B* data. Three layers of large-scale FACs are observed: the downward current with a density of up to $2 \mu\text{A}/\text{m}^2$ located approximately between 77° and 79° latitude, the upward current of comparable density is between 71° and 77° . The radar position closest to the trajectory is in the zone of the current flowing from the ionosphere. The second values of FAC (not shown) reached $10 \mu\text{A}/\text{m}^2$ or more. Such quantities can be registered by the *SWARM* SC over arcs and rays of auroras during substorms [12].

On January 9, 2014, radar observations were carried out according to the SR program in the ipy mode throughout the day. Figure 7a shows successive 1-min vertical Ne profiles measured from 20:21 to 20:38 UT. At 20:29 UT, during substorm activation, when the satellite trajectory crosses the layer of the FAC flowing from the ionosphere, the maximum increase in Ne, up to $8 \times 10^{11} \text{ m}^{-3}$, is observed at *E* layer altitudes of 120 km.

An increase in plasma density to $5 \times 10^{11} \text{ m}^{-3}$ is noticeable in the *F* layer and over its entire height. Analogously to the previous event, Fig. 7b shows three profiles: the central one at 20:29 UT and the profiles averaged over the three previous and three subsequent minutes (the minute of 20:30 UT was omitted as a fault). The difference between the central and neighboring Ne profiles at the maximum *E* layer reaches approximately $5.5 \times 10^{11} \text{ m}^{-3}$. In the *F* layer, this difference is about $2 \times 10^{11} \text{ m}^{-3}$.

3. NUMERICAL EVALUATION OF THE RELATIONSHIP BETWEEN FAC DENSITY AND ELECTRON DENSITY

In the high-latitude ionosphere, FACs are closed by horizontal Pedersen currents. The carriers of the FACs are electrons, and the carriers of ionospheric currents are ions. In the place of the upward FACs, electrons accumulate, and, under the action of the electric field that has arisen here, the ions begin to flow horizontally to this area. On the contrary, the concentration of the ionospheric plasma should decrease in the place of the FACs flowing into the ionosphere. In [6, 8], a quantitative assessment of this phenomenon was made based on the analytical solution of the system of continuity equations for the con-

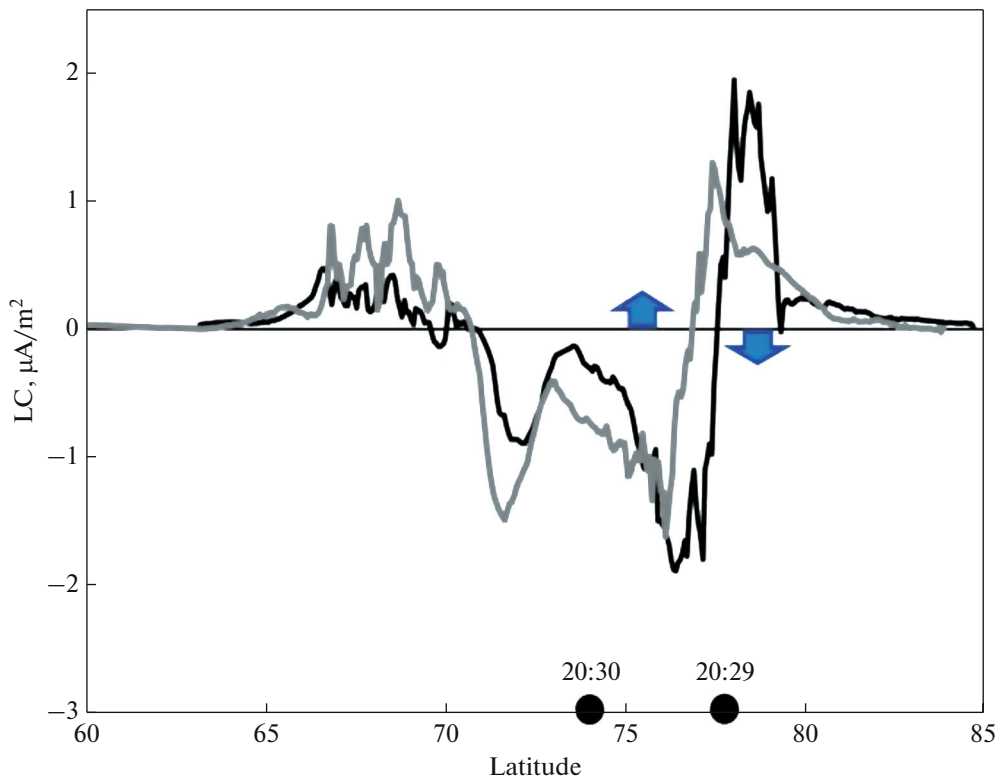


Fig. 6. FAC density according to measurements of *SW-A* (gray line) and *SW-C* (black line) SC for January 9, 2014. An arrow pointing down (up) denotes the FAC inflowing into the ionosphere (outflowing from the ionosphere). Dots on the *X* axis indicate minutes when the *SW-C* SC was close to the ESR.

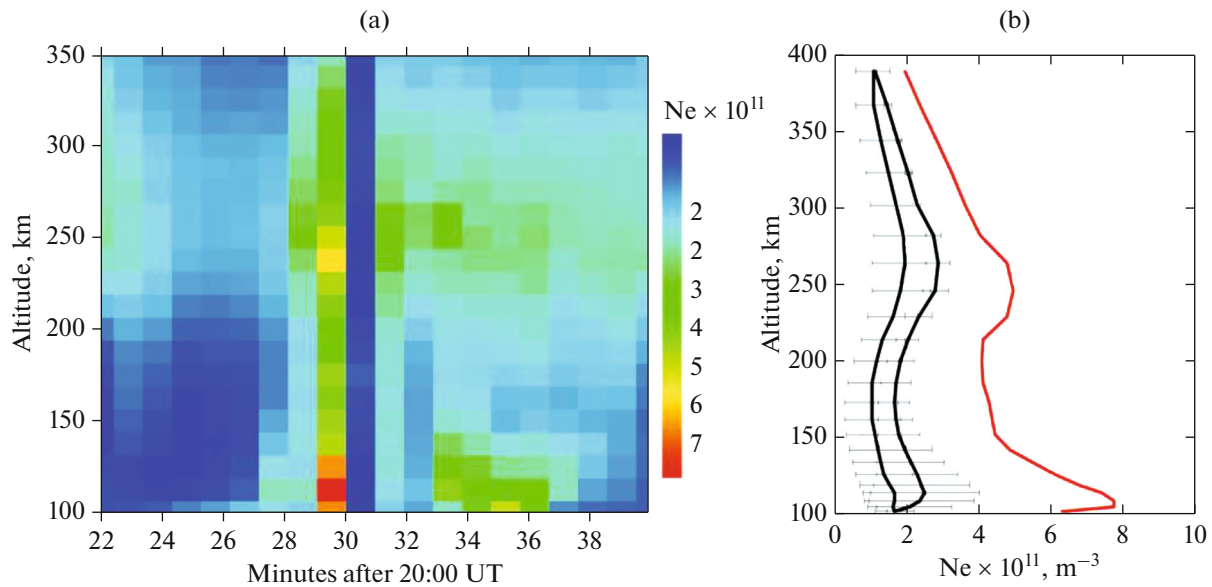


Fig. 7. (a) Altitude distribution of Ne at 20:21–0:38 UT on January 9, 2014; (b) Ne vertical profile at 20:29 UT (red line) and profiles averaged over the three previous and three subsequent minutes (lines with standard deviation).

centration of charged particles and currents and the equation of motion for ions:

$$\begin{aligned}
 Q - \alpha N &= \text{div}(N \times \vec{V}), \quad \text{div}(\Sigma \times \vec{E}) = j_z \\
 e \times \vec{E} + e(\vec{V} \times \vec{B}) - m\vec{v} \times \vec{V} &= 0,
 \end{aligned}
 \tag{1}$$

where Q is the ion-formation rate, α is the recombination coefficient, N is the concentration of ions (one grade is taken into account), \vec{V} is the ion-velocity vector, Σ is the integral conductivity tensor, \vec{E} is the horizontal electric-field strength vector, j_z is the FAC den-

Table 1. Parameter values during the events of February 5, 2017, and January 9, 2014

	February 5, 2017		January 9, 2014	
Geomagnetic conditions	Quiet		Substorm	
MLT of spacecraft flying over the radar beam	~16:30		~21:30	
Measured upward FAC density, $\mu\text{A}/\text{m}^2$	MAX value at 30-s averaging (1-s extremum)			
	0.8 (7.5)		1.8 (12.2)	
Assessment type	Theory	Measurements	Theory	Measurements
E layer ΔN , m^{-3}	2×10^{11}	0.4×10^{10}	4.5×10^{11}	5.8×10^{11}
F layer ΔN , m^{-3}	4×10^{10}	4×10^{10}	4.5×10^{11}	2.3×10^{11}

sity, e is the charge of the ion, \vec{B} is the magnetic-induction vector, m is the mass of the ion, and v is the frequency of ion collisions.

The Pedersen conductivity is defined as

$$\Sigma_p = \frac{e}{B} \int N f(z) dz, \quad (2)$$

$$f(z) = \frac{v}{\omega} \frac{1}{1 + \frac{v^2}{\omega^2}}, \quad (3)$$

where ω is the gyrofrequency and z is height. Based on the given change in the values of v and ω with height, one can calculate the values of function $f(z)$. It reaches its maximum ($f=0.5$) in the E layer on $z=130$ km and decreases to 0.01 per $z=100$ and 300 km. The theoretical estimate of the deviation of altitude profile N_e from the undisturbed profile N_{e0} in taking into account the effect of the FAC for the conditions of the E layer is reduced to the expression

$$\Delta N = 5 \times 10^5 f(z) j_z, \quad (4)$$

and that for the conditions of the F layer to the expression

$$\Delta N = 0.5 j_z N_{e0}. \quad (5)$$

Satellite and radar measurements for the above events give the values of both quantities: ΔN and j_z , which makes it possible to compare the results of measurements and theoretical estimates. A summary of the parameter values measured during satellite flybys over the radar sounding area on February 5, 2017, and January 9, 2014, and the parameter values calculated using relations (4) and (5) is given in Table 1. Note that the values of ΔN calculated for the heights of actually observed maxima of E and F layers located at ~120 and 250 km, respectively. The fact that, according to formula (3), the maximum value of f is at an altitude of 130 km, suggests that the maximum E layer is here. However, according to radar observations, the maximum E layer is located 10–20 km lower. Therefore, the value $f=0.5$ should be applied sooner to the height of the observed maximum, and not to the height of

130 km. We also note once again that, in the first event, conjugate measurements were carried out in quiet geomagnetic conditions and the flyby trajectory over the radar was in the afternoon sector of local time. In the second event, the flight over the radar hit the substorm activation peak and the trajectory passed through the premidnight sector. These significantly different conditions determined the observed large differences in the intensity of the FAC and in the magnitude and nature of the change in N_e .

Comparison of the measured and calculated ΔN values at the maximum E and F layers shows fairly good agreement, at least in order of magnitude, for the event of January 9, 2014, in the nighttime ionosphere under conditions of substorm activation. For the event of February 5, 2017, when measurements were made in the post-noon sector, in the F layer, the measured and calculated values of ΔN match with great accuracy. However, in the E layer, the values of ΔN differ by more than an order of magnitude. The observed values turn out to be much smaller than those predicted by the theory. This discrepancy, presumably, is due to the fact that, during the quiet period, the FAC directed from the ionosphere are carried by the lowest-energy electron fluxes with an energy of no more than a few kiloelectronvolts. Fluxes of precipitating particles significantly depend on the level of geomagnetic activity. The main contribution to ionization in the auroral zone is made by electrons with energies of 1–10 keV. Electrons with energies of 1 keV are absorbed in the F layer, and electrons with an energy of 10 keV are absorbed in the E layer. In the disturbed nighttime ionosphere, carriers of the upwardly directed FAC are represented by the entire energy spectrum, and in the daytime quiet ionosphere, only by its low-energy part. These features are not taken into account in (2)–(3).

4. DISCUSSION

Both events considered above are related to the effect of FAC flowing from the ionosphere and the corresponding local increase in the plasma density. In the case of downward currents, one can expect a local

decrease in Ne, caused by electrons going up. However, this effect is less pronounced, and no events were found in the ESR database in which it would be possible to reliably identify the decrease in Ne associated with the downward FAC. This may be due to the fact that the ionosphere cannot provide an upward flow of electrons (i.e., FAC directed downward) greater than that created by external ionization. A field-aligned electric field may appear, and protons of magnetospheric origin may act as current carriers. The relationship between downward FAC and ion precipitation is not very well studied, since the energy flux of electrons is almost ten times greater than the energy flux of ions (mostly protons), and protons are not the dominant source of energy in the high-latitude region. Previous observations have shown that, as a rule, there is an imbalance between the pair of oppositely directed FAC of regions 1 and 2 on both the dawn and dusk sides. So, on the dusk side, the total upward current of region 1 is greater than the downward current of region 2 (e.g., [13]). Estimation of the effect of the downward FAC on the change in the Ne vertical profile with decreasing ionospheric plasma density requires additional studies using combined radar and satellite observations.

Special radar experiments were carried out mainly in combination with optical ones [14]. However, only direct measurements of the FAC make it possible to estimate the ratio between the FAC density and the local change in Ne. An indirect indicator of Ne variations there may be a change in ionospheric conductivity. In [15], the relationship between the FAC and the integrated conductivity at auroral latitudes was studied. Simultaneous measurements of FAC from space were carried out using the system of *Ampere* satellites and measurements of ionospheric conductivity using the Poker Flat Incoherent Scatter Radar (PFISR), which is the second incoherent scatter radar, after ESR, and is located in Alaska. The results of the correlation analysis showed that there is a closer relationship between the conductivity and the upward FAC as compared to the FAC flowing into the ionosphere. The correlation increases during the night hours and decreases during the noon/dawn MLT hours. This feature may be the result of variations in the average energy of the particle population on the field lines of the auroral geomagnetic field. Electrons with energies less than 1 keV do not contribute significantly to the increase in conductivity, because they produce only a small amount of ionization below 200 km. For auroral particles associated with the FAC and having average energies less than 1 keV, no increase in conductivity was observed, even if the fluxes of precipitating particles increased. Statistical relationships between FAC and ionospheric conductivity from *Ampere* and PFISR data indicate the same effects identified and quantified using combined *SWARM* and ESR observations.

CONCLUSIONS

The results of combined measurements of the *SWARM* spacecraft and the European incoherent scatter radar ESR in Svalbard are analyzed. Vector magnetometers onboard the *SWARM* spacecraft provide measurements of field-aligned current density over the ionosphere. The radar, which is under the flyby trajectory at this time, measures the vertical distribution of electron density Ne.

Two representative events of simultaneous observations, one in the nighttime ionosphere during sub-storm activation and the second in the daytime ionosphere under quiet conditions, showed that the plasma density increases in the place of the field-aligned current flowing from the ionosphere. However, height profile Ne varies in different ways. In the nighttime ionosphere, under disturbed conditions, at the site of the field-aligned current flowing from the ionosphere ($1.8 \mu\text{A}/\text{m}^2$), the plasma density increases in both the *E* layer (up $6 \times 10^{11} \text{ m}^{-3}$) and the *F* layer ($\sim 3 \times 10^{11} \text{ m}^{-3}$). The change in Ne in magnitude is in agreement with the theoretical estimates made on the basis of the solution of the continuity equations. In the daytime quiet ionosphere with an upward current ($0.8 \mu\text{A}/\text{m}^2$), Ne increases only in the *F* layer (on $\sim 4 \times 10^{10} \text{ m}^{-3}$), but practically does not change in the *E* layer. The differences can be due to the fact that, in the first case, the carriers of the upward directed current are represented by the entire energy spectrum of auroral electrons of 1–10 keV, and, in the second case, only by the low-energy part.

ACKNOWLEDGMENTS

The data of the following measuring systems, which are freely available, were used in the work: *SWARM* SC (<http://earth.esa.int/swarm>), ESR radar via the MADRIGAL portal (<http://portal.eiscat.se/madrigal/>), maps of field-aligned currents through the *Ampere* portal (<https://ampere.jhuapl.edu>), and the IMAGE auroral electrojet index (<https://space.fmi.fi/image/www/index.php?#>).

CONFLICT OF INTEREST

The author declares that she has no conflicts of interest.

REFERENCES

1. Iijima, T. and Potemra, T.A., The amplitude distribution of field-aligned currents at northern high latitudes observed by Triad, *J. Geophys. Res.*, 1976, vol. 81, pp. 2165–2174.
<https://doi.org/10.1029/JA081i013p02165>
2. Neubert, T. and Christiansen, F., Small-scale, field-aligned currents at the top-side ionosphere, *Geophys. Res. Lett.*, 2003, vol. 30, no. 19.
<https://doi.org/10.1029/2003GL017808>
3. Lukianova, R., Swarm field-aligned currents during a severe magnetic storm of September 2017, *Ann. Geo-*

- phys.*, 2020, vol. 38, pp. 191–206.
<https://doi.org/10.5194/angeo-38-191-2020>
4. Marklund, G., Auroral arc classification scheme based on the observed arc-associated electric field pattern, *Planet. Space Sci.*, 1984, vol. 32, pp. 193–211.
 5. Aikio, A.T., Lakkala, T., Kozlovsky, A., and Williams, P.J.S., Electric fields and currents of stable drifting auroral arcs in the evening sector, *J. Geophys. Res.*, 2002, vol. 107, no. A12.
 6. Lyatskaya, A.M., Lyatskii, V.B., and Mal'tsev, Yu.P., Influence of field-aligned currents on the electron density profile, *Geomagn. Aeron.*, 1978, vol. 8, no. 2, pp. 229–234.
 7. Deminov, M.G., Kim, V.P., and Khagai, V.V., Influence of field-aligned currents on the structure of the ionosphere, *Geomagn. Aeron.*, 1979, vol. 19, no. 4, pp. 743–745.
 8. Lyatskii, V.B. and Mal'tsev, Yu.P., *Magnitosferno-ionosfernoe vzaimodeistvie* (Magnetosphere–Ionosphere Interaction), Moscow: Nauka, 1983.
 9. Ritter, P. and Lühr, H., Curl-B technique applied to swarm constellation for determining field-aligned currents, *Earth Planets Space*, 2006, vol. 58, pp. 463–476.
<https://doi.org/10.1186/BF03351942>
 10. Lehtinen, M.S. and Huuskonen, A., General incoherent scatter analysis and GUISDAP, *J. Atmos. Terr. Phys.*, 1996, vol. 58, pp. 438–452.
[https://doi.org/10.1016/0021-9169\(95\)00047-X](https://doi.org/10.1016/0021-9169(95)00047-X)
 11. Anderson, B.J., Korth, H., Waters, C.L., et al., Development of large-scale Birkeland currents determined from the active magnetosphere and planetary electrodynamics response experiment, *Geophys. Res. Lett.*, 2014, vol. 41, pp. 3017–3025.
<https://doi.org/10.1002/2014GL059941>
 12. Lukianova, R.Yu., Extreme field-aligned currents during magnetic storms of the 24th solar cycle: March 2015 and September 2017, *Cosmic Res.*, 2020, vol. 58, no. 2, pp. 65–78.
<https://doi.org/10.1134/S0010952520020069>
 13. Le, G., Slavin, J.A., and Strangeway, R.J., Space technology 5 observations of the imbalance of regions 1 and 2 field-aligned currents and its implication to the cross-polar cap Pedersen currents, *J. Geophys. Res.*, 2010, vol. 115, p. A07202.
<https://doi.org/10.1029/2009JA014979>
 14. Sugino, M., Fujii, R., Nozawa, S., et al., Field-aligned currents and ionospheric parameters deduced from EISCAT radar measurements in the post-midnight sector, *Ann. Geophys.*, 2002, vol. 20, pp. 1335–1348.
<https://doi.org/10.5194/angeo-20-1335-2002>
 15. Robinson, R.M., Kaeppler, S.R., Zanetti, L., et al., Statistical relations between auroral electrical conductances and field-aligned currents at high latitudes, *J. Geophys. Res.: Space Phys.*, 2020, vol. 125, p. e2020-JA028008.
<https://doi.org/10.1029/2020JA028008>